Effect of Phosphorylation of Myelin Basic Protein By MAPK on its Interactions with Actin and Actin Binding to a Lipid Membrane in Vitro †

ARTICLE *in* BIOCHEMISTRY · FEBRUARY 2006

Impact Factor: 3.02 · DOI: 10.1021/bi0519194 · Source: PubMed

4 AUTHORS, INCLUDING:

Joan Boggs
SickKids

183 PUBLICATIONS **5,397** CITATIONS

Effect of Phosphorylation of Myelin Basic Protein By MAPK on its Interactions with Actin and Actin Binding to a Lipid Membrane in Vitro[†]

Joan M. Boggs,[*,‡,#] Godha Rangaraj,[‡] Wen Gao,[‡] and Yew-Meng Heng[§]

Division of Structural Biology and Biochemistry, Research Institute, and the Department of Paediatric Laboratory Medicine, Hospital for Sick Children, 555 University Avenue, Toronto, Ontario, Canada M5G 1X8, and the Department of Laboratory Medicine and Pathobiology, University of Toronto, Toronto, Ontario, Canada M5G 1L5

ABSTRACT: Myelin basic protein (MBP) binds to negatively charged lipids on the cytosolic surface of oligodendrocyte membranes and is most likely responsible for adhesion of these surfaces in the multilayered myelin sheath. It can also polymerize actin, bundle F-actin filaments, and bind actin filaments to lipid bilayers through electrostatic interactions. MBP consists of a number of posttranslationally modified isomers of varying charge, some resulting from phosphorylation at several sites by different kinases, including mitogen-activated protein kinase (MAPK). Phosphorylation of MBP in oligodendrocytes occurs in response to various extracellular stimuli. Phosphorylation/dephosphorylation of MBP also occurs in the myelin sheath in response to electrical activity in the brain. Here we investigate the effect of phosphorylation of MBP on its interaction with actin in vitro by phosphorylating the most highly charged unmodified isomer, C1, at two sites with MAPK. Phosphorylation decreased the ability of MBP to polymerize actin and to bundle actin filaments but had no effect on the dissociation constant of the MBP−actin complex or on the ability of Ca^{2+}-calmodulin to dissociate the complex. The most significant effect of phosphorylation on the MBP−actin complex was a dramatic reduction in its ability to bind to negatively charged lipid bilayers. The effect was much greater than that reported earlier for another charge isomer of MBP, C8, in which six arginines were deiminated to citrulline, resulting in a reduction of net positive charge of 6. These results indicate that although average electrostatic forces are the primary determinant of the interaction of MBP with actin, phosphorylation may have an additional effect due to a site-specific electrostatic effect or to a conformational change. Thus, phosphorylation of MBP, which occurs in response to various extracellular signals in both myelin and oligodendrocytes, attenuates the ability of MBP to polymerize and bundle actin and to bind it to a negatively charged membrane.

Myelin basic protein (MBP)[1] is 30% of the total protein and about 10% of the dry weight of myelin. It is bound to the cytosolic side of the oligodendrocyte (OL) membrane, primarily through electrostatic interactions with acidic lipids (reviewed in ref *1*). It is present throughout compact internodal myelin and is probably involved in adhesion of the cytosolic surfaces of the multilayered myelin sheath (*2*, *3*). However, it may have other functions as well. MBP is an intrinsically unstructured protein (*4*−*7*), giving it sufficient flexibility to bind to a charged surface over its entire length and to acquire whatever local conformation is necessary to optimize binding to several different targets. Such proteins are often multifunctional regulatory proteins (*8*). In addition to negatively charged lipids, MBP interacts with polyanions such as actin filaments (*9*−*11*) and microtubules in vitro (*12*) and binds to other ligands such as Ca^{2+}-calmodulin (CaM) (*13*−*15*). Size isoforms of MBP containing the segment encoded by exon II also have been found to localize in the nucleus, where they may bind to polynucleotides (*16*). Jones et al. (*17*) have pointed out that the interaction of proteins with polyanions such as actin is characterized by a lower degree of specificity, albeit high affinity, than for other intermolecular interactions. These interactions may nevertheless be functional.

Another function of MBP may be to interact with the cytoskeleton in oligodendrocytes, in cytosolic inclusions in myelin, and even in compact myelin, where MBP, actin, and tubulin may be associated with the radial component, a series of tight junctions that pass through many layers of myelin (*18*). MBP in solution binds to F-actin in a 1:1 mole ratio and induces the formation of ordered bundles of F-actin filaments (*9*). It also binds to G-actin in solution at an MBP/actin mole ratio of 1:2 and causes its polymerization into filaments under otherwise nonpolymerizing low ionic strength conditions (*10*, *11*).

[†] This work was supported by a grant to JMB from the Canadian Institutes of Health Research.

* To whom correspondence should be addressed: Division of Structural Biology and Biochemistry, Hospital for Sick Children, 555 University Ave., Toronto, ON, Canada M5G 1X8. Tel.: (416) 813-5919. Fax: (416) 813-5022. E-mail: jmboggs@sickkids.ca.

[‡] Division of Structural Biology and Biochemistry, Research Institute, Hospital for Sick Children.

[§] Department of Paediatric Laboratory Medicine, Hospital for Sick Children.

[#] University of Toronto.

[1] Abbreviations: C1, naturally occurring, least modified, most positively charged isomer of 18.5 kDa MBP; C8, least positively charged isomer of MBP with 6 Arg replaced by citrulline; CaM, calmodulin; CMC, carboxy methyl cellulose chromatography; LUVs, large unilamellar vesicles; MAPK, mitogen-activated protein kinase; MARCKS, myristoylated alanine-rich C kinase substrate; MBP, myelin basic protein; MRP, MARCKS-related protein; OLs, oligodendrocytes; P-C1, C1 phosphorylated in vitro by MAPK; PC, phosphatidylcholine; PG, phosphatidylglycerol; PI, phosphatidylinositol.

We showed earlier that MBP could bind actin filaments to the surface of negatively charged lipid vesicles, suggesting that it may be able to act as a membrane actin-binding protein (*19*). This property may allow it to participate in signaling (*20*). Ca^{2+}-calmodulin (CaM) dissociates MBP from actin bundles (*9*) and from actin filaments, resulting in their depolymerization (*10*). CaM-binding also causes dissociation of MBP and the MBP−actin complex from lipid vesicles (*19*, *21*).

MBP (pI ∼ 10) interacts with G-actin and F-actin through electrostatic interactions. These interactions are inhibited by an increase in salt concentration and by a decrease in the net positive charge of MBP due to a variety of posttranslational modifications (*21*, *22*), including substitution of Gln for six Arg (*21*) to mimic a naturally occurring charge isomer, C8, in which six Arg are posttranslationally deiminated to citrulline (Cit) (*23*). This decreases its net positive charge from +19 to +13 at pH 7.4. MBP is also modified in vivo by Ser/Thr phosphorylation (*24*−*26*). Phosphorylation of MBP in the myelin sheath is altered in response to the nerve action potential (*27*−*29*) and in oligodendrocytes in culture in response to extracellular ligands or to depolarization (*20*, *30*−*32*). Phosphorylation increases the β-sheet structure of MBP in solution (*33*, *34*), alters the interaction of MBP with lipid bilayers (*35*), and decreases the ability of MBP to aggregate lipid vesicles (*36*, *37*). MBP is phosphorylated at several sites in vivo including Thr 97 (bovine sequence), one of two sites phosphorylated by MAP kinase in vitro, the other being Thr 94 (*38*−*40*). The region 93−109 (bovine sequence) near a triproline repeat has similarities to synapsin, also an actin-binding protein (*41*). This region also comprises a putative SH3-ligand with PRTP (residues 95−98), a PXXP SH3-target consensus sequence (*42*). In this paper, we have phosphorylated bovine brain C1, the least modified, most highly charged 18.5 kDa isomer of MBP, at Thr 94 and Thr 97 using mitogen-activated protein kinase (MAPK) and studied the interaction of the phosphorylated isomer, P-C1, with actin and its ability to bind actin filaments to lipid surfaces.

MATERIALS AND METHODS

Proteins. The least modified, most highly positively charged 18.5 kDa isomer, C1, was purified from bovine brain MBP as described (*43*). It was phosphorylated with MAPK by adapting the method of Erickson et al. (*38*). Hirschberg et al. (*40*) have recently reported that MAPK phosphorylates MBP at both Thr 94 and Thr 97 and that a singly phosphorylated isomer was not observed after MAPK phosphorylation. Recombinant p42 MAPK was purchased from New England Biolabs and stored at −80 °C. An aliquot (15 μL) containing 1500 units was diluted with 110 μL of 20 mM Hepes at pH 7.5. A solution of ATP (540 nmol/375 μL) was made in the same buffer containing 27 mM magnesium acetate. A solution of 1 mg/0.5 mL C1 in 20 mM Hepes, pH 7.5 was combined with 125 μL of diluted MAPK and 375 μL of ATP solution and incubated at 30 °C for 3 h. An additional 1500 units MAPK and 375 μL of ATP solution was added, and the sample was incubated at 30 °C overnight. It was centrifuged in a Microcon-3 at 14000*g*, 4°C, and the retentate was recovered and assayed for protein by the Peterson assay (*44*) and run on alkaline-urea tube gels as described (*45*). Naturally occurring MBP migrates as several bands on alkaline gels, termed C1, C2, C3, C4, and C5 (Figure 1), and can be fractionated by carboxy methyl cellulose (CMC) chromatography at alkaline pH. C3 and C5 differ from C1 by an increase in negative charge of −2 and −4, respectively. C8, in which six Arg are deiminated to Cit, does not enter the gel and elutes from the CMC column in the void volume. Preliminary trials showed that samples incubated for 3 h with only one addition of MAPK and ATP resulted in two bands migrating similarly to C1 and C3, while the second addition of MAPK and ATP and overnight incubation resulted in varying proportions of two bands migrating similarly to C3 and C5 (Figure 1); most preparations had primarily one band migrating similarly to C5. Thus, the latter most likely had two moles of phosphate per mole of protein. This was confirmed by mass spectrometry which showed that the predominant species after phosphorylation had a molecular weight of 18 524 compared to 18 364 for the starting material, C1. Sham phosphorylation in the absence of enzyme but in the presence of ATP did not affect the migration of C1 on the alkaline gel. Analysis by PAGE on 10% NuPage Bis-Tris gels showed no degradation of P-C1 after phosphorylation. All of the studies reported in this paper were carried out with preparations migrating like C5. However, no difference in behavior from preparations containing a mixture of C3 and C5 was observed.

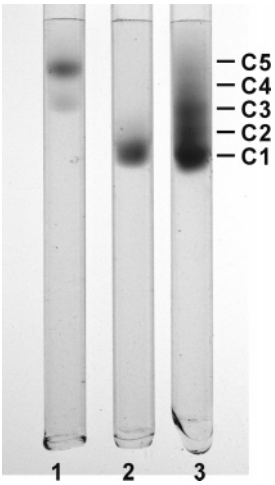

FIGURE 1: Alkaline tube gels of P-C1 (1), C1 (2), and unfractionated bovine MBP (3). The positions of the charge isomers C1, C2, C3, C4, and C5 are indicated, although there is little C4 and C5 in this sample of bovine MBP. Mass spectrometry confirmed that there were two moles of phosphate per mole of P-C1.

Egg L-α-phosphatidylcholine (PC) was purchased from Sigma (St. Louis, MO). L-α-Phosphatidylglycerol (PG; prepared from egg PC) and L-α-phosphatidylinositol (PI) were obtained from Avanti Polar Lipids, Inc. (Alabaster, AL). [^{3}H]-Cholesterol was from Amersham (Baie d'Urfe, QC, Canada).

G-actin and pyrene-labeled actin were purchased from Cytoskeleton (Denver, CO) and stored lyophilized at 4 °C. CaM was purchased from Calbiochem (San Diego, CA). Na2ATP (grade 1) was purchased from Sigma (St. Louis, MO). Rabbit anti-actin antibody was purchased from Sigma (St. Louis, MO), rabbit polyclonal anti-MBP antibody (E5), IgG fraction, was a gift from Dr. E. Day (*46*), and goat anti-rabbit IgG conjugated to HRP was purchased from Jackson ImmunoResearch Labs (West Grove, PA). ECL Western blotting reagents were from Amersham.

Pyrene-Actin Polymerization. Actin polymerization was determined by monitoring the increase in fluorescence of pyrene-actin (*47*). Actin and pyrene-actin were combined in a 10:1 ratio and a solution was made in G buffer (5 mM Tris-HCl, pH 8.0, containing 0.2 mM Na_2ATP, 0.2 mM $CaCl_2$, 0.2 mM DTT, 0.001% TX-100) (*48*) at a concentration of 3 mg/8.1 mL G buffer and was left to stand at room temperature for 1 h. An aliquot was taken for protein assay, and the remainder was centrifuged at 100000*g* in a Ti 70.1 rotor for 1 h at 4 °C to remove any F-actin. Most (80%) of the supernatant was carefully removed, and an aliquot was taken for protein assay by the Bradford method (*49*). An aliquot (at least 275 μL) corresponding to 100 μg (2.3 nmol) of actin was added to a 0.5 mL glass cuvette for each sample. Sufficient G buffer to give a total volume of 0.45 mL was added; the sample was excited at 365 nm, and emission was measured at 407 nm for 5 min. For polymerization due to F buffer, a 50 μL aliquot of a 10× solution of F buffer (0.5 M KCl, 20 mM $MgCl_2$, and 10 mM ATP in G buffer) was then added, the sample was mixed by inversion of the cuvette, and emission was measured for 30 min. For measurement of the dependence of polymerization on the amount of C1 and P-C1 in G buffer, aliquots containing 100 μg of actin (2.3 nmol) were added to test tubes, additional G buffer (to give a total volume of 0.45 mL after subsequent addition of the MBP solutions) was added to the actin, and baseline emission read for 5 min. Aliquots of the MBP solutions were added to the G-actin in the test tubes, the samples were incubated for 45 min at room temperature, and emission was read for 3 min. A 50 μL aliquot of 10× F buffer (5 mM Tris-HCl, pH 8 containing 2 mM $MgCl_2$, 50 mM KCl, 0.2 mM $CaCl_2$, 1 mM Na_2ATP, 0.5 mM DTT, 0.001% TX-100) was then added to each sample, the samples were incubated for 30 min at room temperature, and emission was read for 3 min. (The buffers contained 0.001% TX-100 to inhibit sticking of MBP to glass and plastic tubes as used by Vergères et al. (*50*) for the study of MARCKS-related protein (MRP) with actin.) Under similar conditions, at 4−25 °C, the critical concentration of muscle actin has been reported as 30 μg/mL (*51*). Dobrowolski et al. (*10*) determined that in the presence of MBP, the critical actin concentration was close to zero.

An amount of C1 and P-C1, 15 μg (0.81 nmol), giving less than maximal polymerization was chosen for determination of the rate of polymerization of 100 μg (2.3 nmol) actin in the presence and in the absence of 0.15 M KCl and for determination of the effect of CaM on the rate of depolymerization. For determination of the effect of 0.15 M KCl on polymerization of actin in G buffer, the pyrene-actin (2.3 nmol of actin) was prepared in 0.40 mL of G buffer, 50 μL aliquots of a 1.35 M KCl solution was added, and the emission of the G-actin solution was read for 30−45 min. To determine the effect of MBP in 0.15 M KCl, the pyrene-actin (2.3 nmol of actin) was prepared in 0.385 mL of G buffer, the baseline emission was read for 5 min, and 50 μL of 1.35 M KCl and 15 μg of MBP/15 μL was added. The sample was mixed quickly by inversion, and emission was read every minute for 30−60 min. An aliquot (50 μL) of 10× F buffer was then added to determine fluorescence due to maximum polymerization. For determination of the effect of CaM, the polymerization induced by C1 and P-C1 in G buffer without added KCl was measured similarly except that the total volume of the actin−MBP solution was kept at 0.45 mL. After a steady-state level was reached, 27.5 μL of a CaM solution (1 mg/mL in G buffer) was added to the cuvette, the sample was mixed quickly by inversion, and emission was read until reaching a steady state. In some cases, a 50 μL aliquot of 10× F buffer was then added, the sample was mixed by inversion, and emission was read until the value had plateaued again. The G and F buffers contained 0.2 mM $CaCl_2$; thus, the CaM was in the Ca^{2+}-bound form. The added mole ratio of actin/MBP/CaM was 2.9:1.0:2.0. At the end of the experiment, aliquots were lyophilized and the actin-to-MBP ratio in the samples was analyzed by slot blots.

Slot Blot Analysis. The lyophilized aliquots or pellets after sedimentation were dissolved in 2% SDS, incubated at 37 °C for 15 min, sonicated 2 min at 37 °C, and incubated again at 37 °C for 15 min. They were then diluted with Tris-buffered saline (TBS), and the actin-to-MBP ratio in the pellet was analyzed by slot blots by application of 100 μL of sample to a nitrocellulose membrane, presoaked in TBS, in a Bio-Dot SF Microfiltration system with a 48-well slot format (Bio-Rad Laboratories, Inc., Hercules, CA). The dried membrane was blocked 1.5 h with 5% skim milk in TBS and incubated with anti-actin or anti-MBP Ab in 2.5% milk, followed by incubation with the HRP-conjugated anti-IgG. The membrane was exposed to ECL reagents. Spot densities were analyzed using a UVP-Image Analyzer and compared to those of known amounts of actin and MBP standards to quantify the amount of each protein in the sample.

Electron Microscopy. Actin polymerized in F-buffer, actin−C1 and actin−P-C1 complexes, and actin−C1−LUVs in G or F buffer were used for electron microscopy without centrifugation. A 5 μL droplet of each sample was pipetted onto a Formvar-coated grid and negatively stained with 2% uranyl acetate. The samples were analyzed in a JEM 1230 transmission electron microscope (JEOL USA, Inc.) operated at 80 kV. Digital images of 1024 × 1024 pixels were acquired with a CCD camera (AMT Advantage HR camera system, AMT) attached to the microscope.

Oligodendrocyte Culture and Confocal Microscopy. Rat spinal cord oligodendrocytes were cultured for 7 days, fixed with 4% paraformaldehyde, permeabilized with 0.1% Triton X-100, stained with monoclonal mouse anti-MBP (IgG) specific for residues 131−136 of human MBP (purchased from Sternberger Monoclonals, Inc., Lutherville, MD), donkey Cy™2-conjugated-anti-mouse IgG (from Jackson ImmunoResearch Laboratories, Inc.) and rhodamine-conjugated phalloidin (from Molecular Probes, Eugene, OR), and examined by confocal microscopy as described previously (*52*).

Actin−MBP Sedimentation Assay. The affinities of C1 and P-C1 for F-actin were measured using centrifugation conditions that pellet F-actin plus bound MBP but not free MBP. Aliquots of C1 and P-C1 corresponding to 0.38 nmol of MBP were added to varying concentrations of actin from 0.16 to 4 μM in a total volume of 1 mL of F buffer in ultracentrifuge tubes. The samples were incubated at room temperature for 2 h. They were centrifuged at 100000*g* for 2 h at 4 °C in a Ti 70.1 rotor in a Beckman Optima L-90K ultracentrifuge. The supernatants were removed, and the pellets were analyzed for MBP and actin by slot blots as described above. The concentrations of the C1 and P-C1 stock solutions were

also checked by slot blots. The fractions of bound C1 and P-C1, F_b, were calculated, and the data were fit to the function $A_t = MBP_tF_b + K_dF_b/(1 - F_b)$ according to Yarmola et al. (*53*), where MBP_t is the total C1 or P-C1 concentration and A_t is the total actin concentration.

F-Actin-Bundling Assay. Varying amounts of C1 or P-C1 in F buffer were added to 2 nmol of G actin followed by sufficient F buffer (at least 0.75 mL) to adjust the final volume to 1 mL. The samples were incubated for 30 min at room termperature and centrifuged in an Eppendorf centrifuge at 15000*g* for 15 min to sediment bundled actin filaments, as described (*54*). The supernatants were removed, and aliquots of the supernatant were lyophilized and dissolved in 2% SDS for analysis on slot blots as described above.

Determination of Interaction of Actin and MBP Isomers with Large Unilamellar Vesicles (LUVs). Extruded LUVs of varying lipid composition and containing trace amounts of [^{3}H]-cholesterol were prepared in modified F buffer with the divalent cations omitted, at a final concentration of 1.5 mg of lipid or 1.95 μmol/100 μL as described previously (*19*, *21*, *37*). An amount of 100 μg (5.4 nmol) of C1 or P-C1 in 100 μL of modified G buffer was added to 100 μL of LUVs followed by an aliquot of G-actin solution containing 240 μg of G-actin (5.4 nmol). The sample was incubated at room temperature for 30 min to allow interaction of the proteins before addition of F buffer. Then sufficient F buffer (containing divalent cations; a minimum of 700 μL) was added to bring the total volume to 1.0 mL. The samples were mixed gently and incubated for an additional 30 min at room temperature.

The samples were placed on a discontinuous sucrose density gradient to separate lipid-free actin−MBP complexes from lipid-bound MBP−actin complexes. The gradient was prepared by layering 1 mL each of 40% sucrose, 20% sucrose, 15% sucrose, and 10% sucrose, each made up in F buffer, in 5 mL Beckman Ultra-Clear ultracentrifuge tubes. The samples were centrifuged at 109000*g* for 18 h at 4 °C in a SW 55Ti rotor in a Beckman Optima L-90K ultracentrifuge. The lipid without protein remained in the aqueous layer above the 10% sucrose layer, whereas the lipid with protein sedimented on top of the 10% layer or further into the gradient as opaque bands which could be clearly seen by eye. The position and appearance of the band was noted, each sucrose layer was collected, and the bands were collected separately and diluted with F buffer. After most of the 40% layer was removed, the bottom of the tube was washed out with F buffer to collect any pellet at the bottom. Aliquots were taken for [^{3}H] counting, protein assay, and analysis by slot blots. Protein was assayed by the Peterson method (*44*). Aliquots for slot blots were lyophilized and taken up in 2% SDS.

RESULTS

Comparison of the Ability of C1 and P-C1 to Cause Actin Polymerization and Filament Bundling. Both C1 and its phosphorylated isomer P-C1 caused a rapid increase in fluorescence of pyrene-actin in G buffer, indicating that they caused polymerization of actin (Figure 2A,B). At a 0.5 to 1 mole ratio of C1 to actin, the fluorescence increase is equivalent to that induced by F buffer (containing 2 mM $MgCl_2$ and 50 mM KCl) (*21*), and P-C1 caused a similar increase in fluorescence at this ratio (Figure 3). However,

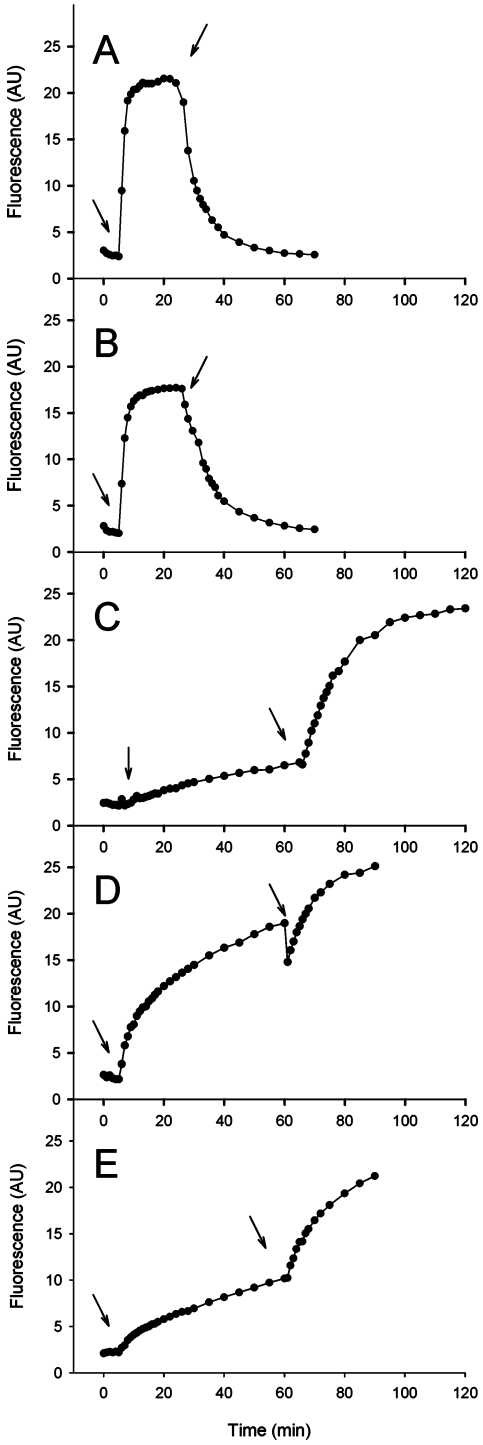

FIGURE 2: (A, B) Time dependence of the increase in fluorescence in arbitrary units (AU) due to polymerization of 2.3 nmol of pyrene−actin induced by 0.8 nmol of MBP isomer and decrease in fluorescence due to depolymerization following dissociation of MBP isomer by 1.6 nmol of CaM for (A) C1 and (B) P-C1. MBP was added at the time indicated by the first arrow and CaM was added at the plateau at the time indicated by the second arrow. (C, D, E) Time dependence of the increase in fluorescence due to polymerization of 2.3 nmol of pyrene-actin in (C) 0.15 M KCl in G buffer, (D) in 0.15 M KCl in G buffer containing 0.8 nmol of C1, and (E) 0.15 M KCl in G buffer containing 0.8 nmol of P-C1. The KCl solution with or without MBP was added at the time indicated by the first arrow. F-buffer was added at the time indicated by the second arrow.

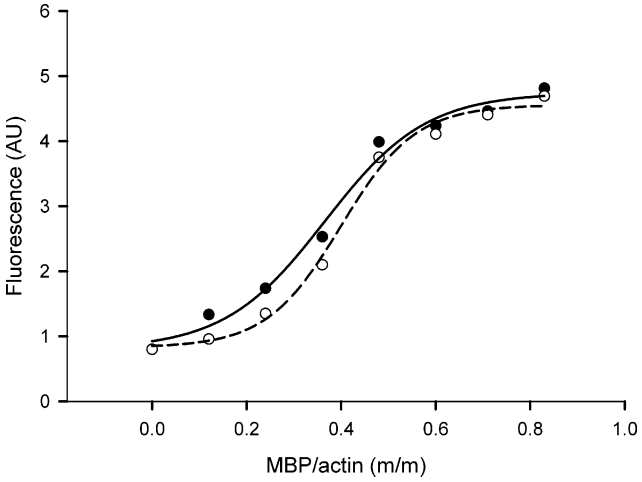

FIGURE 3: Dependence of increase in fluorescence in arbitrary units (AU), due to actin polymerization, on the mole ratio of MBP isomer to actin in G buffer, C1 (closed circles, solid line) and P-C1 (open circles, dashed line). Each sample contained 2.3 nmol of pyrene−actin. Curves were fit to the data by nonlinear regression using a sigmoid 4-parameter equation by SigmaPlot. A representative experiment (of three) is shown.

Table 1: Rate of Actin Polymerization in the Presence of Cl Relative to P-C1[a]

	rate ratio C1/P-C1
actin polymerization in G buffer	1.16 ± 0.13
actin polymerization in G buffer + 0.15 M KCl	2.6 ± 1.4

[a] Rate of polymerization was determined by fit of the first 3−4 data points to a straight line using SigmaPlot Absolute rates varied from one experiment to another depending on the batch of pyrene-actin. However, the differences between C1 and C8 showed the same trend in different experiments. Therefore, the ratios of the rate of Cl-induced polymerization to that of P-C1 from three different experiments were averaged to give the mean rate ratios shown, ± standard deviation.

at lower P-C1-to-actin ratios, the increase in fluorescence was less than that induced by C1 (Figures 2B and 3). The rate of polymerization induced by both isomers was faster than that induced by F buffer, and phosphorylation of C1 did not affect the rate significantly compared to C1 (Table 1). An inflection was observed in the plot of fluorescence vs mole ratio of C1/actin at a mole ratio of about 0.5:1 (Figure 3), consistent with previous reports on a mixture of MBP charge isomers showing that MBP induced maximum polymerization at a MBP/actin mole ratio of 0.5:1 (*9*, *10*). The further increase in fluorescence above this ratio, where the solution became noticeably cloudy, may be due to light scattering due to bundling of actin filaments (*9*, *21*). Because MBP sticks to glass and plastic, the actin−MBP ratios of the combined solutions were checked by analysis on slot blots and confirmed to be identical for each isomer at each of the data points in Figure 3.

Ca^{2+}-CaM causes depolymerization of actin polymerized by MBP (*10*), and it caused more rapid depolymerization of actin in the presence of the less charged recombinant form of C8 than the more positively charged recombinant C1 (*21*). Thus, we compared the rates of Ca^{2+}-CaM-induced depolymerization of actin polymerized by C1 and P-C1 (Figure 2). There was no consistent difference in the rate of Ca^{2+}-CaM-mediated depolymerization in the presence of P-C1 compared to C1 over a number of experiments (not shown).

An increase in ionic strength at 0.15 M KCl decreases the rate of polymerization induced by MBP, indicating that it inhibits the electrostatic interaction between MBP and actin (*21*, *22*). The presence of 0.15 M KCl in G buffer caused much slower polymerization than F buffer (Figure 2C) and significantly slowed the rate of polymerization induced by both isomers in G buffer (Figure 2D,E). The subsequent addition of F buffer caused a more rapid increase in fluorescence, indicating that the higher KCl concentration did not prevent polymerization induced by Mg and ATP. The addition of 0.15 M KCl allowed comparison of the rate of polymerization by C1 and P-C1 under these conditions. The rate of polymerization caused by P-C1 in 0.15 M KCl was significantly less than that by C1 (Figure 2D,E and Table 1).

MBP has been shown to bundle actin filaments (*9*, *10*, *21*, *22*). Electron microscopy showed that most of the F-actin was bundled in the presence of C1, while a significant amount of unbundled actin filaments could be seen in the presence of P-C1, along with bundled actin filaments (Figure 4 A,B,D,E). The actin bundles in the presence of P-C1 appeared thinner and longer than those with C1 (Figure 4A,B) and with little or no branching (Figure 4E) in contrast to those with C1 (Figure 4D). However, P-C1 caused sedimentation of almost as much actin on low speed centrifugation as C1 (Figure 5), indicating that although the actin filaments were bundled by P-C1 more loosely, they were sufficiently cross-linked to sediment at this low speed.

Actin-MBP Binding Assay. Representative equilibrium binding curves from a sedimentation assay of C1 and P-C1 with F-actin after high-speed centrifugation to sediment actin filaments are shown in Figure 6. The dissociation constants for C1 and P-C1 were 51 ± 1 nM and 47 ± 3 nM, respectively (mean of two experiments ± range). Thus, there was no significant difference in the binding affinity of the two isomers for F-actin.

MBP Can Bind Actin to Negatively Charged Lipid Vesicles and is Colocalized with Actin in Oligodendrocytes. MBP binds tightly to acidic lipids through electrostatic interactions, as it does to actin. Our earlier sedimentation analysis (*19*) showed that membrane-bound C1 could also bind to monomeric G and filamentous F-actin. Furthermore, EM shows that C1 bound to PC/PG 4:1 (mol/mol) large unilamellar lipid vesicles (LUVs) binds F-actin bundles to the surface of the LUVs (Figure 4F,G). Similar results were seen in the presence of G buffer (not shown), indicating that C1 could cause polymerization of G-actin and bundling of actin filaments while bound to lipid. Thus, it can simultaneously bind to actin and to a negatively charged lipid surface, suggesting that it may be able to serve as a membrane actin-binding protein.

Although MBP is distributed homogeneously on the cytosolic side of the membrane sheets produced by oligodendrocytes in culture and most of the MBP and actin in oligodendrocytes are not colocalized, Figure 7 c,f shows that some MBP is colocalized with actin, particularly on the edge of the membrane sheets. Thus, MBP may be involved in binding actin to the membrane at these sites where membrane sheet extension occurs.

Comparison of the Ability of C1 and P-C1 to Bind Actin to LUVs. To determine the effect of phosphorylation of C1 on its ability to bind actin to a negatively charged lipid

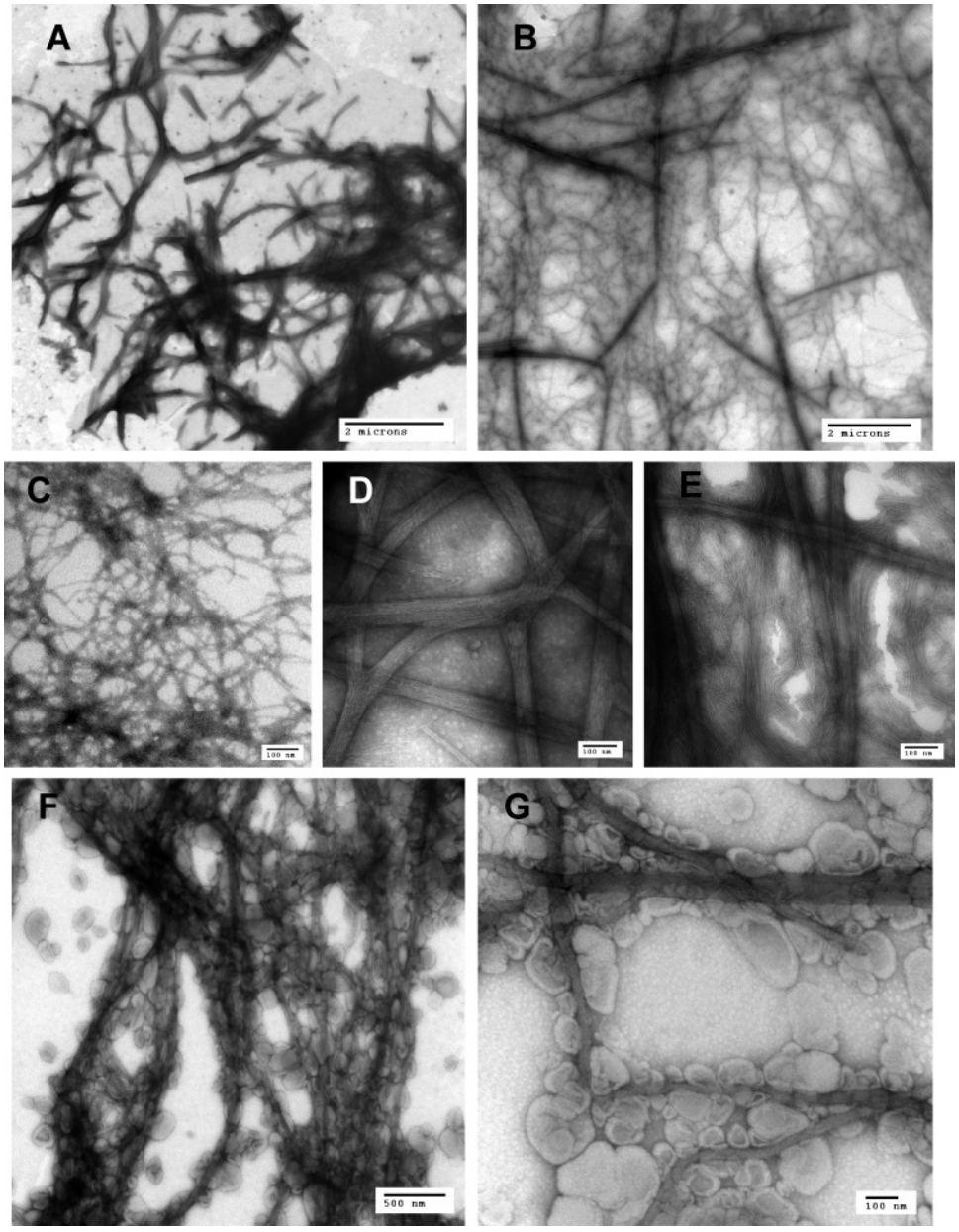

FIGURE 4: Electron micrographs of (A) F-actin in the presence of equimolar C1 in F-buffer, bar = 2 microns; (B) F-actin in the presence of equimolar P-C1 in F-buffer, bar = 2 microns; (C) F-actin in F-buffer, bar = 100 nm; (D) as in (A) but higher magnification, bar = 100 nm; (E) as in (B) but higher magnification, bar = 100 nm; (F) F-actin in the presence of equimolar C1 and PC/PG 4:1 LUVs, bar = 500 nm; (G) as in (F) but higher magnification, bar = 100 nm.

surface, actin and C1 or P-C1 were added to PC/PG or PC/PI LUVs of varying ratio of neutral to acidic lipid. The samples were centrifuged at high speed (109000*g*) on a discontinuous sucrose gradient to separate any actin−MBP complex unbound to lipid from a lipid-bound MBP−actin complex and MBP−lipid or protein-free lipid vesicles. Bands and different sucrose layers were collected, and the amounts of lipid, actin and MBP in each were determined by slot blot analysis as reported previously (*19*, *21*).

Most of the C1 and actin were found bound to lipid vesicles in distinct opaque bands at different sucrose densities. In the absence of C1, actin does not sediment with the lipid vesicles (*19*). The pattern of distribution on the sucrose gradient showed that the samples were heterogeneous (Figure 8). However, more of the lipid and protein, both C1 and actin, sedimented to higher densities as the amount of charged lipid in the vesicles decreased. This is due partly to a greater ability of C1 to aggregate the LUVs and cause their sedimentation, and partly to increased actin binding to the C1−LUVs with a decrease in the surface charge of the LUVs, as reported previously (*37*, *19*). The actin−C1 complex in the absence of LUVs sediments to the bottom of the tube and can be seen as a pellet; 100% of the added protein is recovered in this pellet (*19*). In the presence of LUVs, there was very little C1−actin complex not bound to lipid vesicles at the bottom of the gradient. Some of the actin found at low density for PC/PG 8:2 vesicles (Figure 8A) may have been in solution and not bound to the C1−LUVs, as found previously (*19*), but it was not complexed to lipid-free C1, as the actin−C1 complex would have sedimented to the bottom of the gradient.

The distribution pattern of P-C1 bound to PC/PI 8.5/1.5 LUVs on the gradient was similar to C1 (Figure 8C). However, for LUVs containing more acidic lipid, the

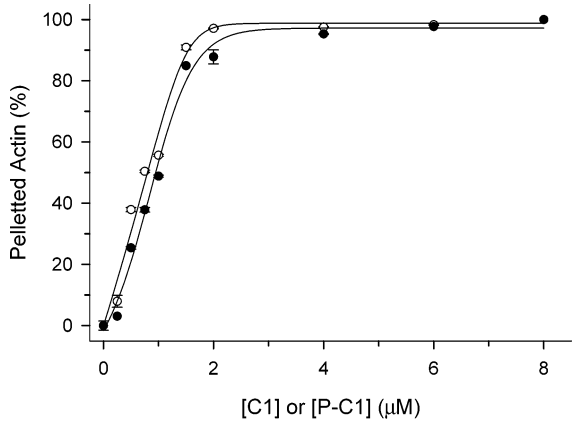

FIGURE 5: Percentage of F-actin (2 μM) pelleted by C1 (open circles) and P-C1 (closed circles) after low-speed centrifugation (15 000 g for 15 min), as determined by slot blots of the amount of actin remaining in the supernatant. The mean ± range of duplicate analyses are shown. Five-parameter sigmoidal curves were fit to the data using SigmaPlot.

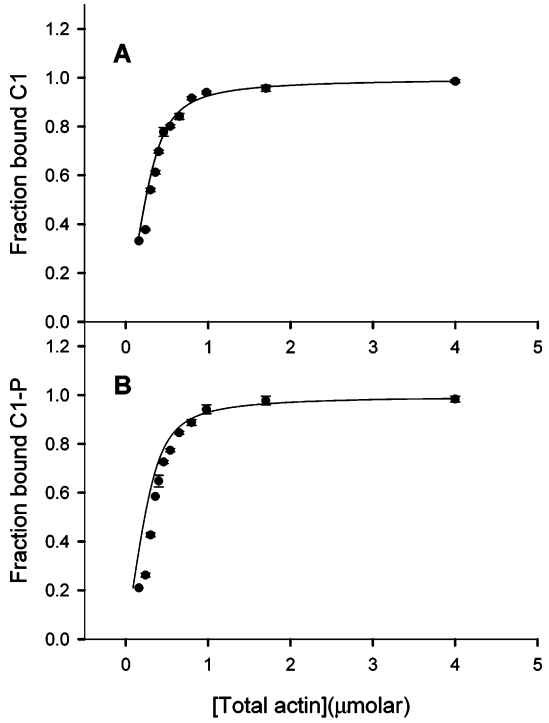

FIGURE 6: Binding of C1 (A) and P-C1 (B) to F-actin determined from a sedimentation assay. Average ± range from an experiment assayed in duplicate is shown. Data were fit assuming a single binding site to the function given in Methods. The fit yielded a k_d of 52.0 nM ($R = 0.996$) for C1 and 50.5 nM ($R = 0.950$) for P-C1. A repeat experiment gave similar results. The mean ± range of the two experiments is given in the text.

distribution pattern of P-C1 on the gradient was distinctly different from C1. In the case of PC/PI 8.25/1.75 LUVs, only 40% of the actin was associated with P-C1-LUVs, mostly in a band containing very little lipid at 40% sucrose (Figure 8B). Another lipid−protein band found at the 20% level contained more lipid and P-C1, but little actin. Most of the actin (60%) and 22% of the P-C1 were found in a protein complex with little lipid at the bottom of the tube. The mole ratio of actin−P-C1 in this complex is 1.1, a little higher than the starting ratio. For PC/PG 8/2 LUVs, almost none of the actin and only 15% of the P-C1 were associated with lipid vesicles (Figure 8A). Most of the actin and P-C1 were found in a protein complex at the bottom of the tube. Thus, P-C1 does not support binding of actin filaments to lipid vesicles at mole percentages of acidic lipid of 17.5% or greater, in contrast to C1. This is not due to a failure of P-C1 to bind to the lipid vesicles. In the absence of actin, all of the P-C1 was bound to PC/PG 8/2 LUVs and caused their sedimentation to the 10% sucrose level, similar to C1 (not shown). However, it is possible that the binding affinity of P-C1 for lipid is less than C1.

DISCUSSION

MBP binds to G-actin and causes its polymerization, and it bundles actin filaments (*9*, *10*). Other highly basic polycationic proteins such as histone, polyamines, fesselin, and calponin (*55*−*58*) and peptides such as the basic effector domain of MRP, similar to that of MARCKS, also increase the rate of polymerization of actin and bundle actin filaments (*53*, *59*, *60*), indicating that electrostatic interactions are a major determinant of actin polymerization and bundling activity. A charge isomer of MBP, rmC8, in which the net positive charge was decreased from +19 to +13 at pH 7.4 (due to Arg-to-Gln substitution in the recombinant form to mimic Arg deimination to Cit in the natural form) had a somewhat lower affinity for F-actin, was dissociated faster by Ca^{2+}-CaM, and did not bundle F-actin as well as the more highly charged isomer rmC1 (*21*). In experiments with lipid-bound actin and natural MBP charge isomers, C8 also did not bind actin filaments to lipid bilayers as well as C1. In contrast to rmC8, P-C1, with a reduction in net positive charge of 2−4, had a similar binding affinity for actin in the presence or in the absence of CaM. However, it significantly decreased the rate of actin polymerization in 0.15 M KCl and did not bundle F-actin as tightly as C1, even at a 1:1 mole ratio, while rmC8 behaved similarly to rmC1 in these respects. EM showed that F-actin bundles in the presence of rmC8 were similar to those in the presence of rmC1 at a 1:1 mole ratio, although light scattering measurements indicated that the ability of rmC8 to bundle actin at lower MBP/actin mole ratios was decreased. The ability of P-C1 to bind actin to LUVs relative to C1 was also diminished more than that of C8. This suggests that phosphorylation at the MAPK sites, Thr 94 and 97, decreased the electrostatic interaction of C1 with actin even more than the loss of six Arg at sites spread throughout the sequence, residues 25, 33, 119, 127, 157, and 168. The greater effect of phosphorylation at Thr 94 and 97 may be due to a concentration of increased negative charge in one domain of the protein. Phosphorylation of C1 inhibits actin polymerization and cross-linking of filaments with each other and with a negatively charged lipid surface but does not inhibit binding to F-actin. This is consistent with earlier studies indicating that MBP has at least two actin-binding sites (*11*). Phosphorylation may interfere with only one of these, while deimination, which is spread over the entire sequence, may interfere with both but in a less severe way.

The reduced ability of P-C1 and C8 to bind actin to negatively charged lipid surface could be partly due to a lower affinity of P-C1 and C8 for the lipid than C1, since some P-C1 and C8 also dissociated with the actin. Although C1, P-C1, and C8 were entirely bound to vesicles with at least 20 mol % acidic lipid in the absence of actin, their binding affinity to lipid has not been measured. C8 and other

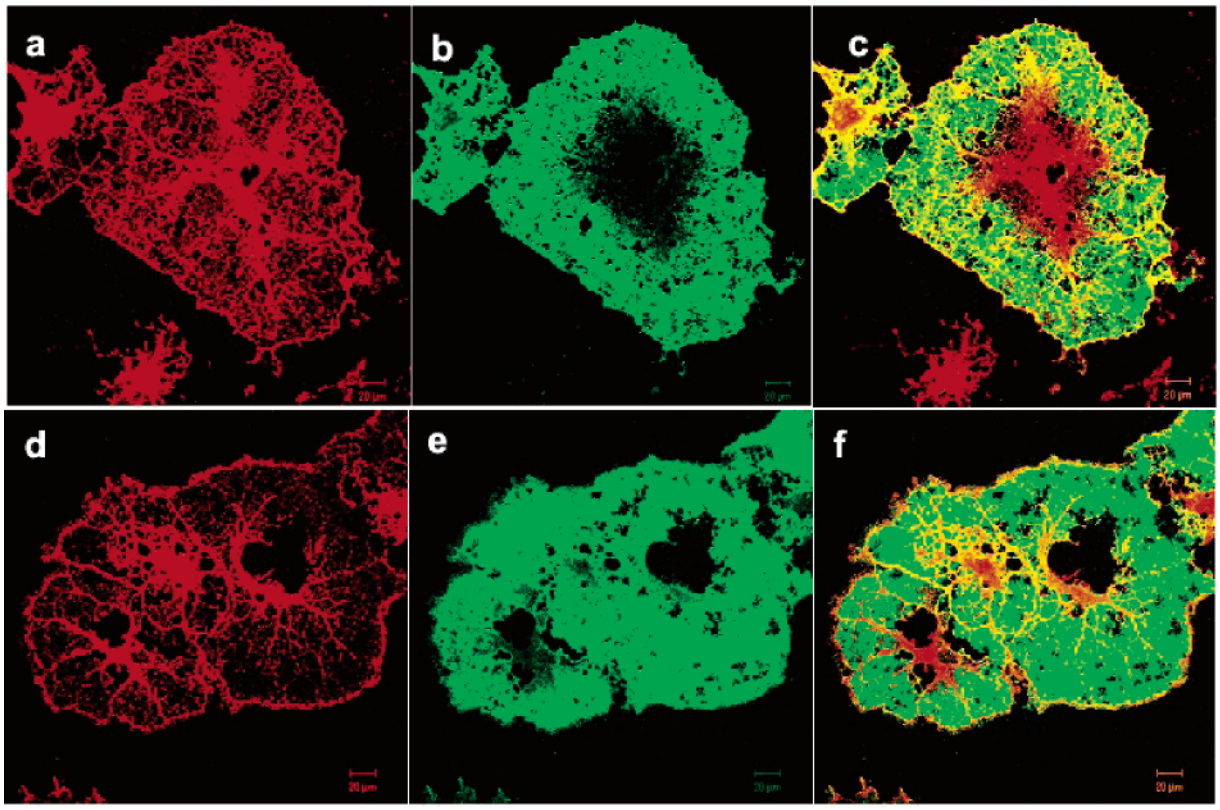

FIGURE 7: Confocal microscope images of cultured oligodendrocytes fixed, permeabilized, and costained with mouse anti-MBP Ab and Cy™2-conjugated-anti-mouse IgG (green) (a, d) and rhodamine-conjugated phalloidin (binds to F-actin) (b, e). Panel (c) is the merged image of a and b, and (f) is the merged image of d and e. Several cells are present in d−f. Two representative images are shown. Colocalization of MBP and actin is seen at the edges of the membrane sheets as well as on veins. Scale bar = 20 μm in each case.

natural charge isomers of MBP, and C1 phosphorylated at a different site by rabbit muscle protein kinase have a reduced ability to aggregate lipid vesicles (*19*, *36*, *37*). A higher net negative surface charge of the bilayer in the presence of the less positively charged P-C1 and C8 would also contribute to reduced actin binding since a more negatively charged surface repels the actin under conditions in which the actin remains bound to lipid-associated C1. An increase in the net negative surface charge of the lipid bilayer due to an increase in the ratio of negatively charged to neutral lipid repels actin, while C1 remains bound to the lipid (*19*). In the case of the MARCKS effector domain, theoretical calculations showed that the electrostatic potential was quite positive above the peptide, even when bound to acidic lipids (*61*). A similar effect for MBP would allow it to bind actin while simultaneously binding to the lipid negative surface charge.

Although the primary function of MBP seems to be to cause adhesion between the cytosolic surfaces of myelin, it may have other functions as well. Polycationic proteins such as MBP can interact with a number of polyanionic proteins and surfaces such as cytosolic membrane phospholipids, actin, microtubules, and polynucleotides (*17*). In addition to actin, MBP can also bind to microtubules in vitro (*12*). Isoforms of MBP containing the segment encoded by exon II have been found to also localize in the nucleus, where they may bind to polynucleotides, whereas the isoforms lacking this segment mainly bind to the cytosolic surface of the membrane (*16*). Such a variety of interactions may play a physiological role, especially for a protein as abundant in OLs and myelin as MBP.

Colocalization studies by immunohistochemistry in immature cultured OLs indicated that MBP is closely associated with microtubules and actin microfilaments (*62*). Here we show that some MBP is also colocalized with actin at the edge of membrane sheets of OLs where it might bind actin to the membrane and participate in membrane sheet extension. MBP might also bind actin to microtubules. In *Shiverer* mouse OLs, which lack MBP, actin microfilaments are not colocalized with microtubular structures as they are in the wild-type OLs (*63*). Compact myelin also contains MBP, actin, and tubulin (*18*, *64*, *65*). They may be associated with the radial component, a series of tight junctions that passes through many layers of compact myelin. They can be isolated in a low density, glycosphingolipid/cholesterol-enriched Triton X-100 insoluble fraction from myelin (*4*−*6*, *62*, *66*), and electron microscopy has shown that this residue from myelin resembles the radial component (*4*). A similar Triton X-100 insoluble fraction from oligodendrocytes resembles intact cytoskeleton (*62*). Thus, MBP-containing membrane domains associated with the cytoskeleton may be present in both myelin and oligodendrocytes.

Phosphorylation of MBP can regulate its ability to bind actin filaments to the lipid membrane. This is an additional regulatory mechanism in addition to those of Ca^{2+}-CaM binding, increase in membrane surface charge, and deimination reported earlier (*19*, *21*). Phosphorylation of a number of membrane actin-binding proteins such as MARCKS, myosin II, annexin II (calpactin I), and synapsin regulates their interaction with the cytoskeleton and the membrane (*54*, *67*−*70*). Both oligodendrocytes and myelin contain several

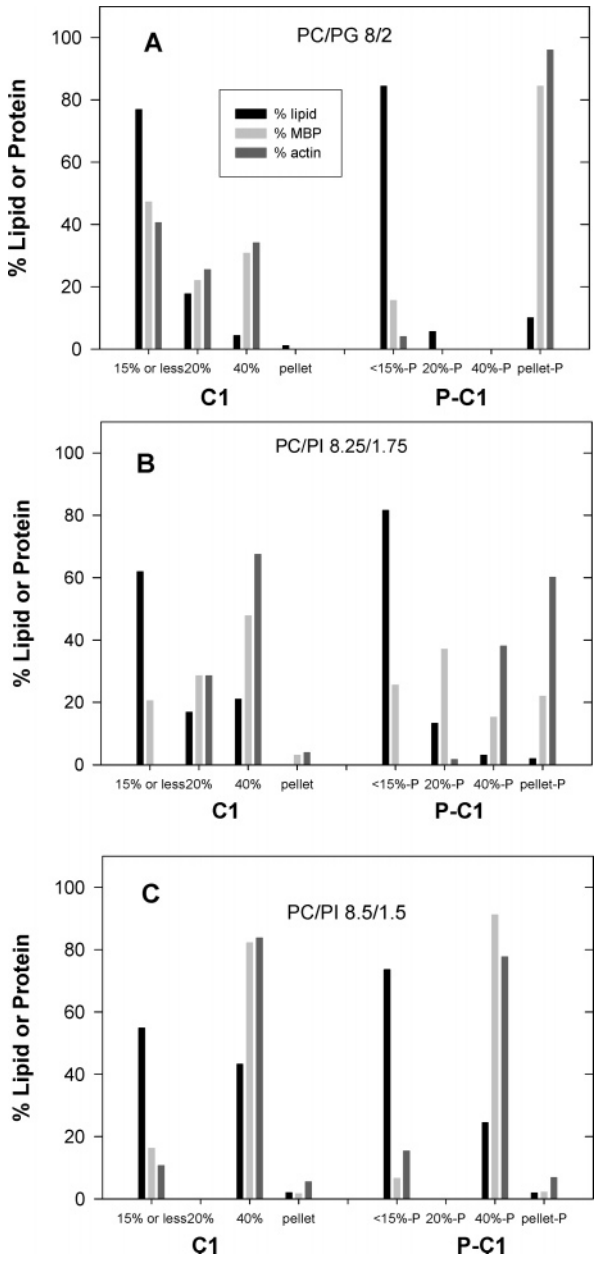

FIGURE 8: Percentage of total amount of lipid (black bar), actin (dark gray bar), and MBP (light gray bar) found in different sucrose density gradient fractions for LUVs of varying ratio of PC to acidic lipid (PG or PI). (A) PC/PG 8/2 LUVs, (B) PC/PI 8.25/1.75 LUVs, and (C) PC/PI 8.5/1.5 LUVs. Data representative of three experiments is shown. The samples were heterogeneous with two or three opaque lipid or lipid−protein bands at different sucrose densities and/or a protein pellet at the bottom of the tube. The amounts shown for sucrose density of 15% or less include amounts in the buffer at the top of the gradient as well as opaque lipid or lipid−protein bands which sedimented into the sucrose density gradient as far down as the 15% sucrose layer. 20% sucrose includes material that sedimented on top of or less than halfway into the 20% sucrose layer. 40% sucrose includes material that sedimented most of the way through the 20% sucrose layer or to the top of the 40% layer. Material that sedimented part way into the 40% layer was also included if some lipid was also present. No opaque bands were seen below the top of the 40% layer. The pellet is material that sedimented to the bottom of the tube. It could be seen as a visible pellet and was recovered after removing all of the sucrose solution and washing out the tube with F buffer. Small amounts of lipid present in this pellet may have been due to contamination from material higher in the gradient. Data for C1 is shown on the left side of each panel and data for P-C1 is shown on the right side of each panel.

kinases that can phosphorylate MBP on Ser and Thr and phosphatases that can mediate rapid turnover of phosphate groups (reviewed in ref *71*). Turnover was highest in the most mature myelin (*72*). We have shown that the p42/p44 MAPK in myelin is active and phosphorylates exogenous MBP (*66*) and endogenous MBP present in a complex with other myelin proteins and MAPK (*73*, W. Min and J. M. Boggs, unpublished). Thus, mechanisms are present in both oligodendrocytes and myelin to regulate the interaction of MBP with actin by phosphorylation.

REFERENCES

1. Boggs, J. M., Moscarello, M. A., and Papahadjopoulos, D. (1982) Structural organization of myelin. Role of lipid−protein interactions determined in model systems, in *Lipid−Protein Interactions* (Jost, P., Griffith, O. H., Eds.) Vol. 2, pp 1−51, John Wiley and Sons, New York.
2. Omlin, F. X., Webster, H. D., Palkovits, C. G., and Cohen, S. R. (1982) Immunocytochemical localization of basic protein in major dense line regions of central and peripheral myelin, *J. Cell Biol. 95*, 242−248.
3. Readhead, C., Takasashi, N., Shine, H. D., Saavedra, R., Sidman, R., and Hood, L. (1990) Role of myelin basic protein in the formation of central nervous system myelin, *Ann. N. Y. Acad. Sci. 605*, 280−285.
4. Uversky, V. N. (2002) Natively unfolded proteins: a point where biology waits for physics, *Protein Sci. 11*, 739−756.
5. Dyson, H. J., and Wright, P. E. (2002) Coupling of folding and binding for unstructured proteins, *Curr. Opin. Struct. Biol. 12*, 54−60.
6. Hill, C. M., Bates, I. R., White, G. F., Hallett, F. R., and Harauz, G. (2002) Effects of the osmolyte trimethylamine-*N*-oxide on conformation, self-association, and two-dimensional crystallization of myelin basic protein, *J. Struct. Biol. 139*, 13−26.
7. Harauz, G., Ishiyama, N., Hill, C. M., Bates, I. R., Libich, D. S., and Fares, C. (2004) Myelin basic protein-diverse conformational states of an intrinsically unstructured protein and its roles in myelin assembly and multiple sclerosis, *Micron 35*, 503−542.
8. Pandey, N., Ganapathi, M., Kumar, K., Dasgupta, D., Das Sutar, S. K., and Dash, D. (2004) Comparative analysis of protein unfoldedness in human housekeeping and non-housekeeping proteins, *Bioinformatics 20*, 2904−2910.
9. Barylko, B., and Dobrowolski, Z. (1984) Ca^{2+}-calmodulin-dependent regulation of F-actin-myelin basic protein interaction, *Eur. J. Cell Biol. 35*, 327−335.
10. Dobrowolski, Z., Osinska, H., Mossakowska, M., and Barylko, B. (1986) Ca^{2+}-calmodulin-dependent polymerization of actin by myelin basic protein, *Eur. J. Cell Biol. 42*, 17−26.
11. Roth, G. A., Gonzalez, M. D., Monferran, C. G., De Santis, M. L., and Cumar, F. A. (1993) Myelin basic protein domains involved in the interaction with actin, *Neurochem. Int. 23*, 459−65.
12. Modesti, N. M., and Barra, H. S. (1986) The interaction of myelin basic protein with tubulin and the inhibition of tubulin carboxypeptidase activity, *Biochem. Biophys. Res. Commun. 136*, 482−489.
13. Grand, R. J. A., and Perry, S. V. (1980) The binding of calmodulin to myelin basic protein and histone H2B, *Biochem. J. 189*, 227−240.
14. Chan, K.-F. J., Robb, N. D., and Chen, W. H. (1990) Myelin basic protein: interaction with calmodulin and gangliosides, *J. Neurosci. Res. 25*, 535−544.
15. Libich, D. S., Hill, C. M. D., Bates, I. R., Hallett, F. R., Armstrong, S., Siemiarczuk, A., and Harauz, G. (2003) Interaction of the 18.5 kDa isoform of myelin basic protein with Ca^{2+}-calmodulin: effects of deimination assessed by intrinsic Trp fluorescence spectroscopy, dynamic light scattering, and circular dichroism, *Protein Sci. 12*, 1507−1521.
16. Pedraza, L. (1997) Nuclear transport of myelin basic protein, *J. Neurosci. Res. 50*, 258−264.
17. Jones, L. S., Yazzie, B., and Middaugh, C. R. (2004) Polyanions and the proteome, *Mol. Cell. Proteomics 3*, 746−769.
18. Karthigasan, J., Kosaras, B., Nguyen, J., and Kirschner, D. A. (1994) Protein and lipid composition of radial component-enriched CNS myelin, *J. Neurochem. 62*, 1203−1213.

19. Boggs, J. M., and Rangaraj, G. (2000) Interaction of lipid-bound myelin basic protein with actin filaments and calmodulin, *Biochemistry 39*, 7799−7806.
20. Dyer, C. A., Philibotte, T. M., Wolf, M. K., and Billings-Gagliardi, S. (1994) Myelin basic protein mediates extracellular signals that regulate microtubule stability in oligodendrocyte membrane sheets, *J. Neurosci. Res. 39*, 97−107.
21. Boggs, J. M., Rangaraj, G., Hill, C. M. D., Bates, I. R., Heng, Y.-M., and Harauz, G. (2005) Effect of arginine loss in myelin basic protein, as occurs in its deiminated charge isoform, on mediation of actin polymerization and actin binding to a lipid membrane in vitro, *Biochemistry 44*, 3524−3534.
22. Hill, C. M. D., and Harauz, G. (2005) Charge effects modulate actin assembly by classic myelin basic protein isoforms, *Biochem. Biophys. Res. Commun. 329*, 362−9.
23. Wood, D. D., and Moscarello, M. A. (1989) The isolation, characterization, and lipid-aggregating properties of a citrulline containing myelin basic protein, *J. Biol. Chem. 264*, 5121−5127.
24. Deibler, G. E., and Martenson, R. E. (1973) Chromatographic fractionation of myelin basic protein. Partial characterization and methylarginine contents of the multiple forms, *J. Biol. Chem. 248*, 2392−2396.
25. Chou, F. C.-H., Chou, C.-H. J., Shapira, R., and Kibler, R. F. (1976) Basis of microheterogeneity of myelin basic protein, *J. Biol. Chem. 251*, 2671−2679.
26. Zand, R., Li, M. X., Jin, X., and Lubman, D. (1998) Determination of the sites of posttranslational modifications in the charge isomers of bovine myelin basic protein by capillary electrophoresis-mass spectroscopy, *Biochemistry 37*, 2441−2449.
27. Murray, N., and Steck, A. J. (1984) Impulse conduction regulates myelin basic protein phosphorylation in rat optic nerve, *J. Neurochem. 43*, 243−248.
28. Atkins, C. M., Chen, S.-J., Klann, E., and Sweatt, J. D. Increased phosphorylation of myelin basic protein during hippocampal long-term potentiation, *J. Neurochem. 68*, 1960−1967.
29. Atkins, C. M., Yon, M., Groome, N. P., and Sweatt, J. D. (1999) Regulation of myelin basic protein phosphorylation by mitogen-activated protein kinase during increased action potential firing in the hippocampus, *J. Neurochem. 73*, 1090−1097.
30. Vartanian, T., Szuchet, S., Dawson, G., and Campagnoni, A. T. (1986) Oligodendrocyte adhesion activates protein kinase C-mediated phosphorylation of myelin basic protein, *Science 234*, 1395−1398.
31. Vartanian, T., Szuchet, S., and Dawson, G. (1992) Oligodendrocyte-substratum adhesion activates the synthesis of specific lipid species involved in cell signaling, *J. Neurosci. Res. 32*, 69−78.
32. Soliven, B., Takeda, M., and Szuchet, S. (1994) Depolarizing agents and tumor necrosis factor-α modulate protein phosphorylation in oligodendrocytes, *J. Neurosci. Res. 38*, 91−100.
33. Ramwani, J. J., Epand, R. M., and Moscarello, M. A. (1989) Secondary structure of charge isomers of myelin basic protein before and after phosphorylation, *Biochemistry 28*, 6538−43.
34. Deibler, G. E., Stone, A. L., and Kies, M. W. (1990) Role of phosphorylation in conformational adaptability of bovine myelin basic protein, *Proteins 7*, 32−40.
35. Cheifetz, S., Boggs, J. M., and Moscarello, M. A. (1985) Increase in vesicle permeability mediated by myelin basic protein: effect of phosphorylation of basic protein, *Biochemistry 24*, 5170−5175.
36. Cheifetz, S., and Moscarello, M. A. (1985) Effect of bovine basic protein charge microheterogeneity on protein-induced aggregation of unilamellar vesicles containing a mixture of acidic and neutral phospholipids, *Biochemistry 24*, 1909−1914.
37. Boggs, J. M., Yip, P. M., Rangaraj, G., and Jo, E. (1997) Effect of posttranslational modifications to myelin basic protein on its ability to aggregate acidic lipid vesicles, *Biochemistry 36*, 5065−5071.
38. Erickson, A. K., Payne, D. M., Martino, P. A., Rossomando, A. J., Shabanowitz, J., Weber, M. J., Hunt, D. F., and Sturgill, T. W. (1990) Identification by mass spectrometry of threonine 97 in bovine myelin basic protein as a specific phosphorylation site for mitogen-activated protein kinase, *J. Biol. Chem. 265*, 19728−19735.
39. Martenson, R. E., Law, M. J., and Deibler, G. E. (1983) Identification of multiple in vivo phosphorylation sites in rabbit myelin basic protein, *J. Biol. Chem. 258*, 930−937.
40. Hirschberg, D., Radmark, O., Jornvall, H., and Bergman, T. (2003) Thr94 in bovine myelin basic protein is a second phosphorylation site for 42-kDa mitogen-activated protein kinase (ERK2), *J. Protein Chem. 22*, 177−181.
41. Pedraza, L. T., Roth, G. A., and Cumar, F. A. (1988) Identification as synapsin of a synaptosomal protein immunoreacting with anti-myelin basic protein antiserum, *J. Neurochem. 51*, 413−420.
42. Moscarello, M. A. (1997) Myelin basic protein, the "executive" molecule of the myelin membrane, in *Cell Biology and Pathology of Myelin: Evolving Biological Concepts and Therapeutic Approaches* (Juurlink, B. H. J., Devon, R. M., Doucette, J. R., Nazarali, A. J., Schreyer, D. J., Verge, V. M. K., Eds.) pp 13−25, Plenum, NY.
43. Cheifetz, S., Moscarello, M. A., and Deber, C. M. (1984) NMR investigation of the charge isomers of bovine myelin basic protein, *Arch. Biochem. Biophys. 233*, 151−160.
44. Peterson, G. L. (1977) A simplification of the protein assay method of Lowry et al. which is more generally applicable, *Anal. Biochem. 83*, 346−356.
45. Deibler, G. E., Martenson, R. E., and Kies, M. W. (1972) Large scale preparation of myelin basic protein from central nervous tissue of several mammalian species, *Prepr. Biochem. 2*, 139−165.
46. Boggs, J. M., Samji, N., Moscarello, M. A., Hashim, G. A., and Day, E. D. (1983) Immune lysis of reconstituted myelin basic protein−lipid vesicles and myelin vesicles, *J. Immunol. 130*, 1687−1694.
47. Kouyama, T. K., and Mihashi, K. (1981) Fluorimetry study of N-(1-pyrenyl)iodoacetamide-labelled F-actin. Local structural change of actin protomer both on polymerization and on binding of heavy meromyosin, *Eur. J. Biochem. 114*, 33−38.
48. Kaufmann, S., Kas, J., Goldmann, W. H., Sackmann, E., and Isenberg, G. (1992*)* Talin anchors and nucleates actin filaments at lipid membranes. A direct demonstration, *FEBS Lett. 314*, 203−205.
49. Bradford, M. M. (1976) A rapid and sensitive method for the quantitation of microgram quantities of protein utilizing the principle of protein-dye binding, *Anal. Biochem. 72*, 248−254.
50. Vergères, G., Manenti, S., Weber, T., and Sturzinger, C. (1995) The myristoyl moiety of myristoylated alanine-rich C kinase substrate (MARCKS) and MARCKS-related protein is embedded in the membrane, *J. Biol. Chem. 270*, 19879−19887.
51. Gordon, D. J., Boyer, J. L., and Korn, E. D. (1977) Comparative biochemistry of non-muscle actins, *J. Biol. Chem. 252*, 8300−8309.
52. Boggs, J. M., and Wang, H. (2001) Effect of liposomes containing cerebroside and cerebroside sulfate on cytoskeleton of cultured oligodendrocytes, *J. Neurosci. Res. 66*, 242−253.
53. Yarmola, E. G., Edison, A. S., Lenox, R. H., and Bubb, M. R. (2001) Actin filament cross-linking by MARCKS: characterization of two actin-binding sites within the phosphorylation site domain, *J. Biol. Chem. 276*, 22351−22358.
54. Bubb, M. R., Lenox, R. H., and Edison, A. S. (1999) Phosphorylation-dependent conformational changes induce a switch in the actin-binding function of MARCKS, *J. Biol. Chem. 274*, 36472−36478.
55. Grant, N. J., Aimar, C., and Oriol-Audit, C. (1983) Supramolecular forms of actin induced by polyamines; an electron microscopic study, *Eur. J. Cell Biol. 30*, 67−73.
56. Grazi, E., Magri, E., and Pasquali-Ronchetti, J. (1982) Multiple supramolecular structures formed by interaction of actin with protamine, *Biochem. J. 205*, 31−37.
57. Tang, J. X., Szymanski, P. T., Janmey, P. A., and Tao, T. (1997) Electrostatic effects of smooth muscle calponin on actin assembly, *Eur. J. Biochem. 247*, 432−440.
58. Beall, B., and Chalovich, J. M. (2001) Fesselin, a synaptopodin-like protein, stimulates actin nucleation and polymerization, *Biochemistry 40*, 14252−14259.
59. Wohnsland, F., Schmitz, A. A. P., Steinmetz, M. O., Aebi, U., and Vergères, G. (2000) Interaction between actin and the effector peptide of MARCKS-related protein. Identification of functional amino acid segments, *J. Biol. Chem. 275*, 20873−20879.
60. Tang, J. X., and Janmey, P. A. (1996) The polyelectrolyte nature of F-actin and the mechanism of actin bundle formation, *J. Biol. Chem. 271*, 8556−8563.
61. Murray, D., Arbuzova, A., Hangyas-Mihalyne, G., Gambhir, A., Ben-Tal, N., Honig, B., and McLaughlin, S. (1999) Electrostatic properties of membranes containing acidic lipids and adsorbed basic peptides: theory and experiment, *Biophys. J. 77*, 3176−3188.
62. Wilson, R., and Brophy, P. J. (1989) Role for the oligodendrocyte cytoskeleton in myelination, *J. Neurosci. Res. 22*, 439−448.

63. Dyer, C. A., Philibotte, T. M., Billings-Gagliardi, S., and Wolf, M. K. (1995) Cytoskeleton in myelin-basic-protein-deficient shiverer oligodendrocytes, *Dev. Neurosci. 17*, 53−62.
64. Pereyra, P. M., Horvath, E., and Braun, P. E. (1988) Triton X-100 extractions of central nervous system myelin indicate a possible role for the minor myelin proteins in the stability in lamellae, *Neurochem. Res. 13*, 583−595.
65. Gillespie, C. S., Wilson, R., Davidson, A., and Brophy, P. J. (1989) Characterization of a cytoskeletal matrix associated with myelin from rat brain, *Biochem. J. 260*, 689−696.
66. Arvanitis, D. N., Min, W., Gong, Y., Meng, Y.-M., and Boggs, J. M. (2005) Two types of detergent-insoluble, glycosphingolipid/cholesterol-rich membrane domains in isolated myelin, *J. Neurochem. 94*, 1696−1710.
67. Yumura, S., and Kitanishi-Yumura, T. (1992) Release of myosin II from the membrane-cytoskeleton of Dictyosteilium discoideum mediated by heavy-chain phosphorylation at the foci within the cortical actin network, *J. Cell Biol. 117*, 1231−1239.
68. Powell, M. A., and Glenney, J. R. (1987) Regulation of calpactin I phospholipid binding by calpactin I light-chain binding and phosphorylation by p60v-src, *Biochem. J. 247*, 321−328.
69. Hubaishy, I., Jones, P. G., Bjorge, J., Bellagamba, C., Fitzpatrick, S., Fujita, D. J., and Waisman, D. M. (1995) Modulation of annexin II tetramer by tyrosine phosphorylation, *Biochemistry 34*, 14527−14534.
70. Ceccaldi, P. E., Grohovaz, F., Benfenati, F., Chieregatti, E., Greengard, P., and Valtorta, F. (1995) Dephosphorylated synapsin I anchors synaptic vesicles to actin cytoskeleton: an analysis by videomicroscopy, *J. Cell Biol. 128*, 905−912.
71. Ledeen, R. W. (1992) Enzymes and Receptors of myelin, in *Myelin: Biology and Chemistry* (Martenson, R. E., Ed.) pp 531−570, CRC Press, Boca Raton, FL.
72. Ulmer, J. B., and Braun, P. E. (1986) In vivo phosphorylation of myelin basic proteins: age-related differences in ^{32}P incorporation, *Dev. Biol. 117*, 493−501.
73. Arvanitis, D. N., Yang, Y., and Boggs, J. M. (2002) Myelin proteolipid protein, basic protein, the small isoform of myelin-associated glycoprotein, and p42 MAPK are associated in the Triton X-100 extract of central nervous system myelin, *J. Neurosci. Res. 70*, 8−23.

BI0519194